Proceedings of the International Association for Shell and Spatial Structures (IASS) Symposium 2009, Valencia
Evolution and Trends in Design, Analysis and Construction of Shell and Spatial Structures
28 September – 2 October 2009, Universidad Politecnica de Valencia, Spain
Alberto DOMINGO and Carlos LAZARO (eds.)

Finite element simulation of fracture strength of PTFE coated glass fiber fabric membranes

Tatsuya YOSHINO*, Shiro KATO[a],

*Technical Research Center, R&D Division, Taiyo Kogyo Corporation
3-20, Syodai-Tajika, Hirakatashi, Osaka 573-1132, Japan
Email yt003051@mb.taiyokogyo.co.jp

[a] Toyohashi University of Technology
E-mail kato@tutrp.tut.ac.jp

Abstract

In the present study, the theory for the constitutive equation based on Fabric Lattice Model is extended to study the mechanism of fracture under arbitrary bi-axial tensions. Since the former constitutive equations can treat the viscosity, the extended constitutive equations based on the Fabric Lattice Model can be applied to various structural problems and phenomena from tensioning process of membranes to failure of large membrane structures. The study here is first to add the fracture criteria to the previous constitutive equations, second to evaluate the constants added for the fibers inherent to fracture, and finally, based on the extended theory to evaluate the fracture strength under various ratios of bi-axial tensions.

Keywords: Membrane material, Constitutive equation, Visco-elasto-plastic characteristics, Fracture strength, Finite element method, Bi-axial tension test

1. Introduction

Membranes for structure are tensioned in the two directions, and the necessity arises to investigate the fracture or strength capacity under bi-axial and shear deformations. Several studies have been performed by Minami [1] and Komatsu [2] with respect to the fracture of structural membranes with cutouts. However, there are few researches [3,4] for fracture of structural membranes without cutouts. Komatsu [3] investigated the fracture mechanism of PTFE coated glass fiber textile using the conceptual model of fabric membranes. From the study, the fracture strength of the material under equal bi-axial tensions was estimated about 58 to 66% of the fracture strength under uni-axial tension. H. W. Reinhard also obtained the fracture strength of polyvinyl chloride coated polyester fabrics under bi-axial

tensions from experiments [4]. In his study the testing methods were evaluated to see which is best as a material test for fracture among three testing methods; one is a fracture test of materials with flat circular shape, the second is the fracture test of materials using cylinder shape, and the last is a flat square membrane under biaxial tensions. And he concluded that the third testing method is best for finding the fracture strength and this testing method has been adopted by the Membrane Structure Association of Japan (MSAJ) as standard testing for Elastic Constants of Materials [5]. However, during the test adopted by MSAJ, the materials are often found to be fractured at the portions around feet of long arms or at fixing bolts, not at the central part of tested materials, and their true fracture strength are learned not easy to get based on this testing method.

H. W. Reinhard has applied the following method for fracture strength test, where a square fabric membrane is prepared with elongated skirts of a same width, the skirts looking are made artificially sliced in the long direction as shown in Figures.9 and 10, and bi-axial tensions are provided in test. In the test, several ratios of bi-axial tensions were assigned as (1:1), (2:1), (10:1) and others with a larger tension given to the warp direction. It was reported that the fracture strength for the ratios of (1:1), (2:1) and (10:1) corresponds to the fracture strength for the warp and the fracture strength for the ratio of (0:1), (1:10) corresponds to the fracture strength for the weft.

For development of more realistic constitutive equations in FEM analysis, the present authors have proposed a fabric lattice model [6-8] to evaluate the constitutive equations of PTFE glass fiber fabric membranes. And they have proven the validity through comparison between the evaluated constitutive equations and experiments in case of various ratios of bi-axial tensions. Then, the constitutive equations have been implemented into FEM formulation using curved elements, and many simulations [10] have been performed for analysis of stresses and deformations. For examples, analysis of membranes under simultaneous actions of a concentrated load and internal pressure was performed and compared with experiments [7], and also as a simulation [9,10] for introducing stresses into membranes was discussed together with a consideration of viscosity of the materials [6].

In the present study, the theory for the constitutive equation based on Fabric Lattice Model is extended to study the mechanism of fracture under arbitrary bi-axial tensions. Since the former constitutive equations can treat the viscosity, the extended constitutive equations based on the Fabric Lattice Model can be applied to various structural problems and phenomena from tensioning process of membranes to failure of large membrane structures. The study here is first to add the fracture criteria to the previous constitutive equations, second to evaluate the constants added for the fibers inherent to fracture, and finally, based on the extended theory to evaluate the fracture strength under various ratios of bi-axial tensions.

2. Extension of Fabric Lattice Model to fracture problems

The Fabric Lattice Model (FLM) has been validated through the studies [6-8]. The physical components are shown in Figure.1 and the fundamental theory to derive the Model is referred to the papers [6-8], and the added parts are to be explained here with emphasis on the hysteretic rules fiber components.

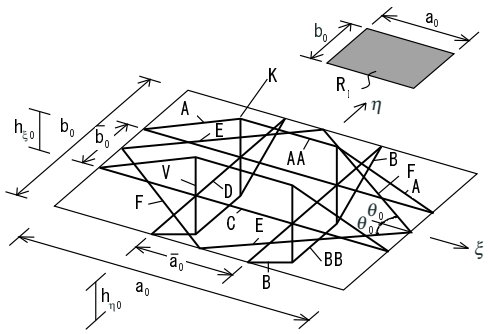

Figure 1 Fabric Lattice Model

2.1 Warp and weft (elements A, AA, B and BB)

The Fabric Lattice Model has been validated through the studies [6-8]. The physical components are shown in Figure.1 and the fundamental theory to derive the Model is referred to the papers [6-8], and the added parts for fracture are to be explained here with emphasis the hysteresis rules of fiber elements.

With increase of tensions given to a membrane sheet, the stresses of fibers are also increased and, after some slacks will disappear, the rigidity becomes higher, and finally the fibers will fracture accompanied with loss of strength and rigidity. Accordingly, the hysteresis rules are assumed for yarns and weft as shown in Figure.2.

2.2 Struts connecting warp and weft (element V)

The strut connects the warp with weft, and the hysteresis rule is applied as given in Figure.3, where no fractures are assumed and the stiffness is increased with compression without any resistance against tension.

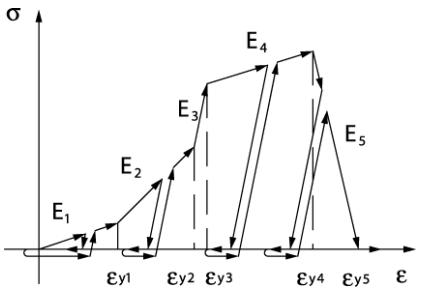

Figure.2 Warp and Weft

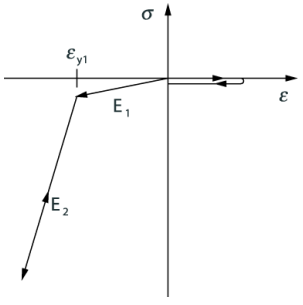

Figure.3 Struts

2.3 Coating elements (elements C, D, E and F)

Coating materials have resistance against tensions and compressions as well as shears, and the hysteresis rules are assumed shown in Figure.4 as a type of tri-linear curves with deterioration and lose the resistance beyond critical deformations.

2.4 Coating element packed between warp and weft （element R_I）

The material is assumed to resist against shear stress because it is packed between warp and weft. The type of hysteresis as shown in Figure.5 is almost same as those for coating materials, and it loses the resistance beyond a critical shear deformation.

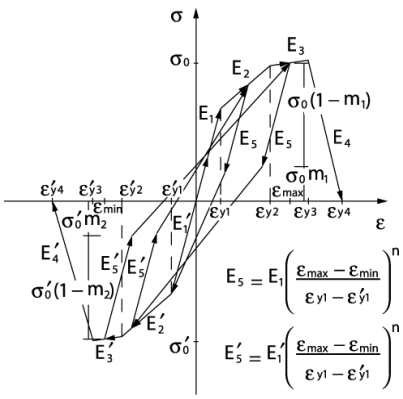

Figure.4 Coating materials

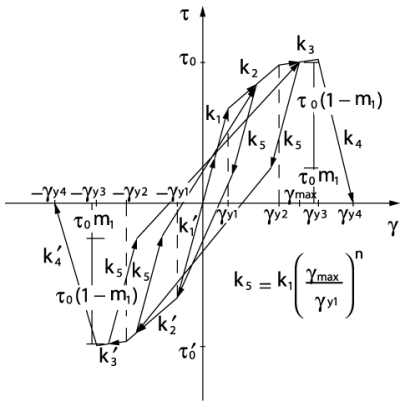

Figure.5 Coating material between yarns

3. Material constants of composing elements

The material constants are based on the previous researches performed by experiments, and they are given in Table. 1. The data were derived from PTFE glass fiber fabric membranes under uni-axial tension test using the material sampled from a same lot. The fracture strength and strains were measured from tested materials of 30mm initial width. The constants of critical strain corresponding to fracture are determined under an assumption that, due to critical large deformations within warp and weft, they lose their resistance and at the same time the coating material lose also the resistance. The critical strains of the composing elements for constitutive equations are thus determined so that they are matched with those of fracture tests under a PTEF of warp direction with a stress ratio of (1:0) and of weft direction with a stress ratio (0:1). The matching was a little difficult and several trials were repeated to reach a convergence. In the trials, the constants of coating materials for shear deformation were kept unchanged. Combining with the constants previously obtained, the data were finally determined as shown in Tables.2 and 3. The constants of negative slopes giving hysteresis after fracture were assumed considering the stability of analysis without referring to the experiments. And the fracture shear strains for coating materials were assumed 100% without matching with experiments.

Table.1 Fracture test under uni-axial test (Experiment)

	Fracture strength (N/30mm)	Fracture strain (%)
Warp	5460	8.8
Weft	4780	15.9

Table.3 Visco-elastic constants from test

	T_g (sec)	C_1 (mm²/kN)	T_1 (sec)	C_2 (mm²/kN)	T_2 (sec)
C	6240000	0.0063	42	0.199	21006
D	3471600	0.0534	220	0.2153	9522
V	255120	1.4153	1400	1.6867	104160

Table.2 Material properties: dimensions and constants for Fabric Lattice Model

Elements		A,AA	B,BB	C		D		E,F		V
A_0	(mm2)	0.16/2	0.16/2	0.40/2		0.40/2		0. 14		0.25/4
ℓ_0	(mm)	0.470	0. 371	1.375		1.000		1.700		0.175
E_1, E'_1	(kN/mm)	0.001	0.001	33.32	33.32	30.87	30.87	5.0	5.0	0.03
E_2, E'_2	(kN/mm)	27.98	27.98	13.23	8.82	12.25	12.25	0.002	0.002	31.36
E_3, E'_3	(kN/mm)	279.8	279.8	6.66	1.96	3.92	3.92	0.001	0.001	-
E_4, E'_4	(kN/mm)	0.001	0.001	-294	-294	-294	-294	-9.8	-9.8	-
E_5, E'_5	(kN/mm)	-392	-294	-		-		-		-
ε_{y1}, ε'_{y1}	(%)	0.001	0.001	0.3	-0.06	0.3	-0.35	0.2	-0.2	-11
ε_{y2}, ε'_{y2}	(%)	0.3	0.3	1.2	-1.2	0.7	-0.7	1.0	-1.0	-17
ε_{y3}, ε'_{y3}	(%)	4.1	5.17	6.0	-6.0	7.0	-7.0	2.0	-2.0	-
ε_{y4}, ε'_{y4}	(%)	4.11	5.18	-		-		-		-
n	-	-	-	0.0		0.0		0.0		-
m_1	-	-	-	0.07		0.08		0.0		-
m_2	-	-	-	0.5		0.5		0.0		-

Elements	k_1 (kN/cm)	k_2 (kN/cm)	k_3 (kN/cm)	k_4 (kN/cm)	γ_{y1}, γ'_{y1} (%)	γ_{y2}, γ'_{y2} (%)	γ_{y3}, γ'_{y3} (%)	n	m_1
R_I	0.0637	0.0304	0.0142	-98	1.66	3.5	100	-0.4	-0.25

4. Fracture strength and fracture stress

Based on the material constants given in Tables 2 and 3, the stress-strain relationships are obtained in the cases of stress ratio for (1:0), (0:1), and (1:0). The results are shown in Figure.6. The fracture strength and strains obtained from analysis are summarized in Table.4, depending on the stress ratio. Fracture stress is measured in real length after deformation, while the fracture strength is measured in nominal length before deformation.

Figure.6 reveals that the membrane under a stress ratio of (1:1) loses the resistance at the peak stress of 157.2N/mm due to the fracture of weft, and that the strain of the weft at the fracture point corresponds to 98.4% of the stress of the weft. The results of fracture strength in each direction are of almost same to those already obtained by H W Reinhardt [4], as shown by the comparison between analysis and experiment in Table.4. Other cases of different stress ratio are also given in Figure.7, where the fracture interaction is given with two different curves. Point A corresponds to stress ratio of (1:0), while Point B to stress ratio of (0:1) and Point C to the stress ratio of (1:1). Point D corresponds to the stress ratio of (1.11: 1), and the stresses are 175.4N/mm and 156.8N/mm respectively, and the strains are 3.8% in the warp direction and 11.7% in the weft direction. At this stress ratio, both the warp and weft rapture at the same time. We here notice that Point D dose not coincides with the stress ratio of (1:1), and it is why not only the density but also the looseness as well as crimp heights are different between the warp and weft directions. The fracture strength of 174.5N/mm under equal bi-axial tensions is 95.8% of the fracture strength of 182.1N/mm under uni-axial strength in the warp direction and 98.2% of the fracture strength under uni-axial strength in the weft direction. Along the range between Points B and D, the membrane reaches its fracture in the weft, while along the range between Points A and D the membrane reaches its fracture in the warp.

The fracture strength along warp changes by 4.2% from the fracture strength under uni-axial stress in the warp, and by 1.8% from the fracture strength under uni-axial stress in the weft. The reference will be, as already estimated, due to the difference of crimp heights in the two directions and due to material characteristics of structural elements of A, B, C, D, E, and F. First, the effect of crimp heights on the fracture strength is analyzed; as shown in the mechanism in the section of fabrics, the fibers reach their fracture at the stress when the stress coincides with $P_y / \cos\theta$, where P_y is the fracture strength of fiber itself, and θ is the slope angle determined by crimp height. Under un-axial test, the angle θ becomes smaller than that under bi-axial stresses while P_y remains constant, and accordingly, the fracture stress will be accounted smaller than those in case of bi-axial stresses.

On the other hand, a consideration is focused on the coating materials, C and D. The directions of elements C and D are same as those of warp and weft, in other word A and B, respectively. As expected from the hysteresis rules in Figure.4, the stresses of elements C and D vary depending on the magnitude of strains, and they increase along with increasing strains up to on the magnitude of the strain ε_{y3}. The fracture strains in the warp direction for the stress ratios (1:0) and (1.11:1) are 5.8% and 3.8%, respectively. The fracture strains in the weft direction for the stress ratios (1:0) and (1.11:1) are 13.0% and 11.7%,

respectively. In both cases, when the stress ratio approaches to the ratio (1.11:0), not only the fracture strains but also fracture stresses in both directions tend to become smaller.

Accordingly, the stresses of elements E and F change depending on both strains in the warp and weft directions, The fracture warp stress in case of stress ratio (1.11:1) is 95.8% of the fracture warp strength in case of stress ratio (1:0). and accordingly it is decreased by 4.2%. If focused on the fracture strain in case of stress ratio (1.11:1), the $\cos\theta$ of the warp is 0.972, and it decreases by 2.8%, that is (1-0.972), in the fracture strength. This decrease will be due to crimp interchange. Since the stress in the warp direction corresponds to the sum of the stresses in the two different groups; a group of (A and AA) and a group of (C, D , E and F), it is estimated that the stress of the coating material (elements C, D, E and F) is decreased by the remaining fraction, 1.4% given as (0.042-0.028) . Similar analysis will be possible in case of weft direction, and the value of $\cos\theta$ of the weft is 0.983 corresponds almost to 1.7% decrease due to the crimp effect.

Here we notice again that the magnitude of the fracture strength is measured with the transverse length before deformation, and the interaction of fracture strength is shown in Figure.7, showing also the fracture stresses measured with the transverse length after deformation. The magnitudes of fracture stresses are a little smaller than those of fracture strength due to deformation of sections; it is why the warp is elongated by 3.2% and 11.8% in the warp and weft directions respectively at the fracture instance.

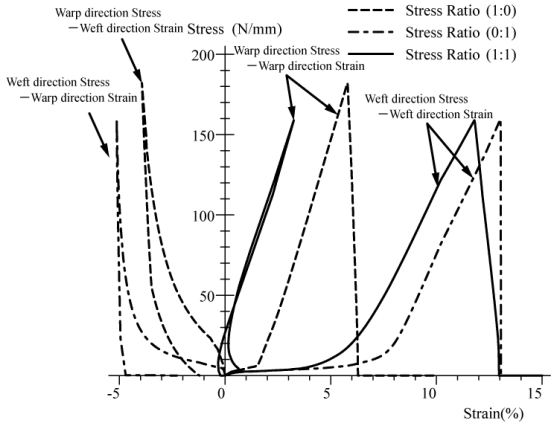

Figure.6 Stress-Strain curves in the case of strain ratio for(1:0),(0:1),(1:1) by FLM

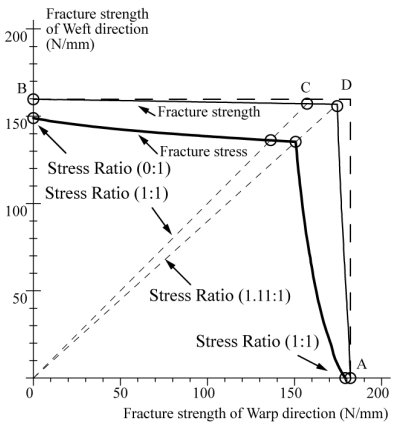

Figure.7 Fracture interaction by FLM

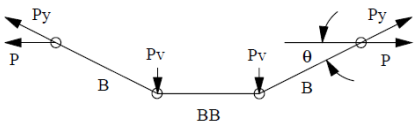

Figure.8 Equilibrium considering crimp interchange (Elements B and BB)

Table.4 Comparison of analysis and experiment with fracture strength (N/mm) and strains

		Analysis based on FLM				Experiments			
		Fracture Strength		Fracture strain (%)		Fracture Strength		Fracture strain (%)	
Point	dir.	Warp	Weft	Warp	Weft	Warp	Weft	Warp	Weft
A	ratio (1:0)	182.1 (100)	0	5.8	-3.9	182.0	-	8.8	-
B	ratio (0:1)	0	1597 (100)	-5.1	13	-	159.3	-	15.9
C	ratio (1:1)	157.2 (88.1)	157.2 (98.4)	3.2	11.8	-	-	-	-
D	ratio (1.11:1)	175.4 (95.8)	156.8 (98.2)	3.8	11.7	-	-	-	-

(The numerrals in the bracket show the ratio in % of anlysis to fracture strength.)

5. Simulation for fracture under biaxial tensions

5.1 Analysis model

To simulate the fracture, the test piece shown in Figure.9 is analyzed using the extended method based on Fabric Lattice Model [6-8].

The shape of pieces for test is based on the MSAJ standard [5]. The analysis is based on 8 node isoparametric curved elements by taking the effects of fracture characteristics and viscosity. The integration for FEM is performed with 2 by 2 Gaussian scheme. The analysis model is shown in Figure.10, and by making use of the symmetric shape, one forth the tested pieces is used in analysis. The boundary condition is provided to match the experiment under bi-axial tensions. The attachments for fixing the pieces at the ends of the tested membrane are also modeled in analysis to move simultaneously and transversely of the neighboring attachment. The loads are given in a condition compatible with the boundary condition. The fracture is judged to appear when any of Gaussian points within any element reaches the fracture from which for stresses to decrease sharply.

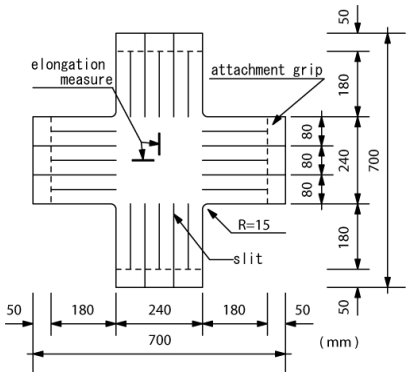

Figure.9 Test piece under test

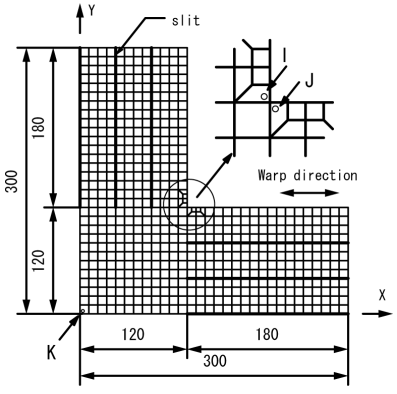

Figure.10 Analysis model

5.2 Results in case of tress ratio (1:1)

The stress distributions at fracture are shown in Figure.11 together with the stress at the central point K. In the FEM analysis the fracture is found to appear at Gauss point I in Figure.10 and the fracture strength as applied forces per 1mm given at the grip ends is summarized in Table.5.

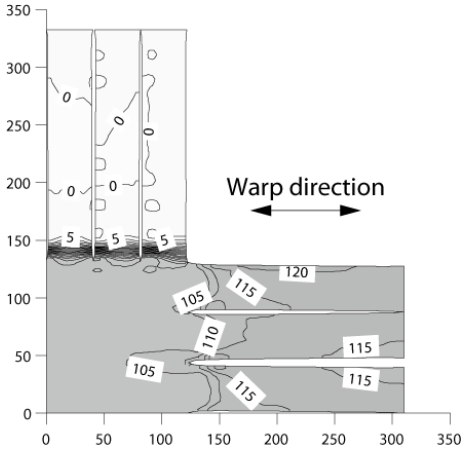

a) Stress in the warp (N/mm)

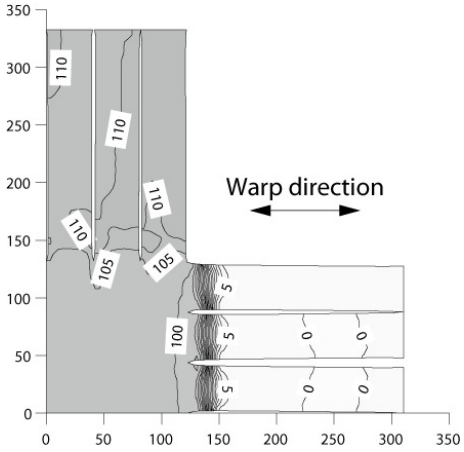

b) Stress in the weft (N/mm)

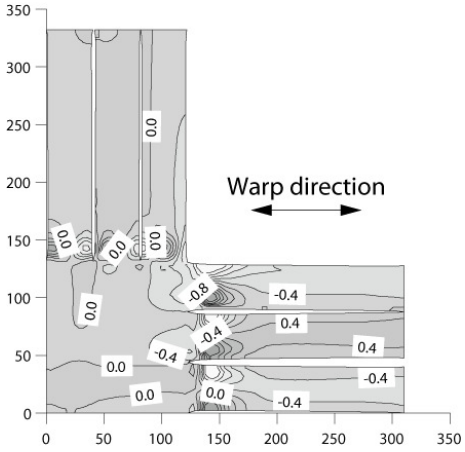

c) Shear Stress (N/mm)

Figure.11 Stress distribution (stress ratio (1:1))

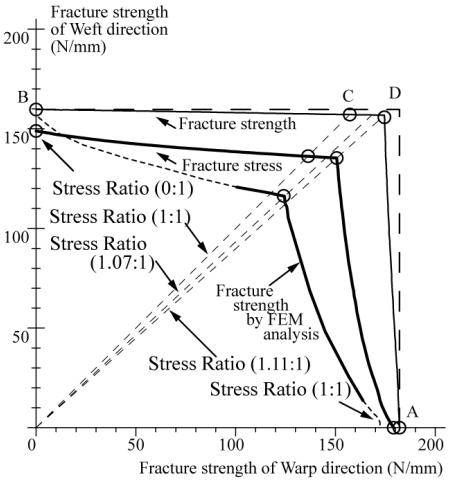

Figure.12 Fracture Strength interaction by FLM and FEM analysis

Table 5 Fracture strength based on FEM analysis and FLM (N/mm)

Fracture strength of test	Fracture strength	Warp	117.7	137.2	145.1	124.9
		Weft	117.7	68.6	48.4	112.4
		ratio	1:1	2:1	3:1	1.11:1
	Stress of integration point I or J	Warp	52	143.9	140.7	156.5
		Weft	145.3	37.3	30.3	49.5
		Point	I	J	J	J
	Stress of integration point K	Warp	103.2	122.7	131.8	109.6
		Weft	103.2	60.5	42.9	98.4
		ratio	1.00:1	2.03:1	3.07:1	1.11:1
Fabric Lattice Model	Fracture strength	Warp	157.2	177.4	179.0	174.5
		Weft	157.2	88.7	59.7	156.8
	Fracture stress	Warp	136.2	157.4	161.6	151.3
		Weft	136.2	78.7	53.9	135.2

The fracture strength is 117.7N/mm(FEM) for the piece under uni-axial tension in the warp direction, and the magnitude is 74.9% of the fracture strength 157.2N/mm(FLM) under equal bi-axial tensions. The stress distribution is found to be moderately smooth due to separated slits at the grip, however, stress concentration is found around points of I and J. The fracture stress at the central point K is 103.2N/mm(FEM) for both direction and this value is only 87.7% of the fracture strength for the case under equal bi-axial tensions. From this simulation, fracture starts at point I with 74.9% of the fracture strength of piece under bi-axial tensions.

5.3 Results in case of tress ratios from (120:1) to (1:120)

The fractures are investigated using FEM analysis for various stress ratios from (120:1) to (1:120). The results are given in Figure.12. The cases of (120:1) to (120:10) for a lager warp component and of (10:120) to (1:20) for a larger weft component give a deformation in analysis that the neighboring attachments get involved and contact each other. On the other hand, in experiment the attachment could not move and could not purchase the movement assumed in analysis, and such deformation of being involved each other is not found in experiment. Due to a fact that the attachment could not move smoothly gave some more stress concentration at the part of fracture and reduced the fracture strength. And this lead a result that as clearly found in Figure.12 the fracture strength is lower in every case than the analytical one based on Fabric Lattice Model.

Along the points of B, C and D in Figure.12, the membrane is judged to reach the fracture due to the fracture of weft, and the changing point from weft fracture to warp fracture is the stress ratio of (1.11:1) in case of analysis, on the other hand, the stress ratio of (1.07:1) in case of experiment.

The fracture strength and fracture stresses at Gauss points I or J and the central point K are given in Table.5. The data correspond to the stress ratio of (2:1), (3:1) and (1.11:1).

It is ascertained from these results that, although the stress at the central point K is a little smaller than other points, the ratio of the appearing stress at point K to the applied load at the attachment is almost same as those in experiment.

6. Conclusions

The previously proposed theory for constitutive equations based on Fabric Lattice model is extended to include the phenomena for viscosity as well as fracture losing the resistance beyond critical deformation. The present constitutive equations have made it possible to accurately simulate many different kinds of behavior from stretching process of membranes at sites to creep, relaxation and fracture experiments at laboratories.

In this paper, simulation for fracture test has been performed and the interaction of fracture strength under various ratio of stress ratio was clearly obtained. Moreover, the testing scheme adopted in MSAJ cords was re-analyzed based on both of FEM Fabric Lattice Model and experiments, and the relationship between the fracture test and the test of MSAJ cords were again investigated in clear sense. Based on the analytical results, the stress at the center of tested pieces could not reach the fracture strength defined at the ends of attachment.

Accordingly, the preset study has clearly pointed out a fact that a more refinement is required to approach a true testing scheme to obtain the fracture strength under bi-axial tensions and to establish a more refine simulation for global analysis of fabric menbrane structures.

References

[1] H. Minami, H. Toyoda, K. Kotera and S. Segawa, “Some Reviews on Methods for Evaluation of Performance of Membrane Materials Being used for Membrane Structures”, Proc. IASS Symp. Vol.2, Osaka, pp.201-208, 1986

[2] K Komatsu : Study on Reliability of Membrane Structure Buildings (Part I) (Study on Breaking Properties of Membrane Materials) , Research Report on Membrane Structures ‘88, The Membrane Structures Association of Japan, No.2, pp.51-64, 1988.12 (In Japanese)

[3] K Komatsu, K Ishii : Simulation of stress deformation of membrane materials having cracks using a woven structure model, Research Report on Membrane Structures ‘92, The Membrane Structures Association of Japan, No. 6, pp.45-78, 1992.12 (In Japanese)

[4] H. W. Reinhardt : On the Biaxial Testing and Strength of Coated Fabrics, EXPERIMENTAL MECHANICS, Vol. 16, No. 2, pp.71-74, February, 1976

[5] The Membrane Structures Association of Japan : Testing Method for Elastic Constraints of Membrane Materials (MSAJ/M-02-1995), Standard of Membrane Structures Association of Japan, 1995

[6] S Kato, H Minami, T Yoshino, T Namita: Analysis of Membrane Structures Based on Fabric Lattice Model Considering Viscous Characteristics, Proceedings of the IASS International Symposium '97 on Shell & Spatial Structures, Singapore, pp.411-420, November 10-14, 1997.

[7] S Kato, H Minami, S Segawa, T Yoshino: Experimental and Analytical Study on Visco-elasto-plastic Characteristics of PTFE-coated Glass Fiber Fabric under Cyclic Loadings, Proceedings of the Lightweight Structures in Architecture, Engineering and Construction IASS/IEAust/LSAA International Congress, Sydney, Australia, pp.800-806, October 5-9, 1998.

[8] Shiro Kato, Tatsuya Yoshino, Hirokazu Minami: Formulation of constitutive equations for fabric membranes based on the concept of fabric lattice model, Engineering Structures 21, pp.691-708, 1999.

[9] S Kato, T Yoshino, H Minami and S Segawa: Study on the Construction Process of Membrane Structures Considering Visco-elasto-plastic Analysis, 40th Anniversary Congress of the International Association for Shell and Spatial Structures, Madrid, pp.C1.93-C1.102, 20-24 September, 1999.

[10] S Kato, T Yoshino: Simulation for Introducing Tensions into Curved Membranes Considering Both of the Cutting Pattern Method and Visco-Elasto-Plastic Characteristics of the Fabrics, International Symposium on Theory, Design and Realization of Shell and Spatial Structures, Nagoya, Japan, TP046, pp178-179, October 9-13, 2001.

[11] T Yoshino, S Kato : Analytical Estimation for Strength of Membrane Materials under the Biaxial Tensions, Research Report on Membrane Structures 2002, The Membrane Structures Association of Japan, No. 16, pp.1 -6, 2002.12 (In Japanese)

[12] T Yoshino, S Kato : Numerical Simulation of the Biaxial Tension Test for Strength of Membrane Materials, Research Report on Membrane Structures 2003, The Membrane Structures Association of Japan, No. 16, pp.1 -5, 2003.12 (In Japanese)